Biochemical Journal (2019) **476** 951–963
https://doi.org/10.1042/BCJ20180831

PORTLAND PRESS

Research Article

Proline residues in scavenger receptor-BI's C-terminal region support efficient cholesterol transport

Sarah C. Proudfoot[1] and **Daisy Sahoo**[1,2,3]

[1]Department of Biochemistry, Medical College of Wisconsin, Milwaukee, WI, U.S.A.; [2]Department of Medicine, Division of Endocrinology, Metabolism & Clinical Nutrition, Medical College of Wisconsin, Milwaukee, WI, U.S.A.; [3]Cardiovascular Center, Medical College of Wisconsin, Milwaukee, WI, U.S.A.

Correspondence: Daisy Sahoo (dsahoo@mcw.edu)

High-density lipoproteins (HDLs) facilitate reverse cholesterol transport, a process in which HDL removes cholesterol from circulation and carries it to the liver for biliary excretion. Reverse cholesterol transport is also facilitated by HDL's high-affinity receptor, scavenger receptor-BI (SR-BI), by mechanisms that are not fully understood. To improve our understanding of SR-BI function, we previously solved the NMR (nuclear magnetic resonance) structure of a peptide encompassing amino acids 405–475 of SR-BI. This segment of SR-BI, that includes the functionally critical C-terminal transmembrane domain and part of the extracellular domain, also contains four conserved proline (Pro) residues. We hypothesized that these proline residues support SR-BI in a conformation that allows for efficient cholesterol transport. To test this, we generated individual Pro-to-alanine mutations in full-length SR-BI and transiently expressed the mutant receptors in COS-7 cells to measure the effects on SR-BI-mediated cholesterol transport functions. Our findings reveal that HDL cell association and uptake of HDL-cholesteryl esters are impaired by mutation of Pro-412, Pro-438, or the transmembrane proline kink residue (Pro-459). In addition, SR-BI-mediated cholesterol efflux and membrane cholesterol distribution are impaired by mutation of Pro-412 or Pro-438, indicating that these residues are essential for a fully functional SR-BI receptor. Furthermore, we demonstrate that Pro-408 is necessary for proper SR-BI expression, but mutation of Pro-408 does not cause SR-BI to become misfolded or rapidly degraded by the proteasome or the lysosome. We conclude that key proline residues play an important role in SR-BI function by allowing for the efficient transport of cholesterol between cells and HDL.

Introduction

Approximately one in three deaths (30.8%) in the U.S.A. are cardiovascular disease-related [1]. Most cardiovascular disease events result from atherosclerosis where cholesterol accumulates in lesions along the artery wall, a process that can progressively occlude vessels and decrease blood flow (reviewed in ref. [2]). High-density lipoproteins (HDLs) protect against atherosclerosis by removing excess cholesterol from circulation via reverse cholesterol transport [3]. During reverse cholesterol transport, HDL accepts cholesterol from cells in the periphery (e.g. arterial macrophages) [4] via cholesterol efflux and transports it to the liver as cholesteryl esters (CEs) via non-endocytic selective uptake of HDL-CE [5]. Once internalized by the liver, CEs are eventually converted to bile and excreted from the body.

Bidirectional cholesterol transport between cells and HDL occurs by a receptor-mediated process involving HDL's high-affinity receptor, scavenger receptor-BI (SR-BI) [4,6]. SR-BI is an 82 kDa cell surface glycoprotein consisting of a large extracellular domain anchored by two transmembrane domains [7]. Since SR-BI is responsible for cholesterol transport, it is important to understand its role

Received: 23 October 2018
Revised: 22 February 2019
Accepted: 5 March 2019

Accepted Manuscript online: 5 March 2019
Version of Record published: 22 March 2019

Biochemical Journal (2019) **476** 951–963
https://doi.org/10.1042/BCJ20180831

in the context of atherosclerosis. SR-BI's role in protecting against atherosclerosis is supported by mouse models in which overexpression of SR-BI in the liver reduces atherosclerosis [8], while whole-body deficiency of SR-BI accelerates atherosclerosis and raises HDL-cholesterol [9]. In humans, rare variants of SR-BI (S112F, T175A, and P297S) were identified in patients with high HDL-cholesterol [10,11], and these mutations significantly impaired *in vitro* SR-BI-mediated cholesterol transport [11,12]. Another rare variant of SR-BI (P376L) is associated with an increased cardiovascular disease risk in humans [13] and mimics phenotypes observed for mice deficient in SR-BI [9]. Altogether, these studies suggest a critical role for SR-BI in reverse cholesterol transport and protection against atherosclerosis; however, the precise mechanisms by which SR-BI facilitates cholesterol transport remain undefined.

The use of structure–function studies has expanded our knowledge of SR-BI cholesterol transport functions [14–18]. Homology models of SR-BI's extracellular domain provided physical evidence of a hydrophobic cavity that can spatially accommodate cholesterol molecules [19]. This evidence supports one hypothesis for SR-BI-mediated cholesterol transport, in which SR-BI transports HDL-CE into cells via a hydrophobic channel that facilitates the movement of CE down its concentration gradient [20]. SR-BI oligomerization may also play a role in cholesterol transport [21,22]. Gaidukov et al. [23] demonstrated that a glycine dimerization motif within the N-terminal transmembrane domain of SR-BI is required for lipid uptake and SR-BI homo-dimerization. We observed homo-dimerization of SR-BI's C-terminal region in live cells using fluorescence resonance energy transfer experiments [24]. Dimerization of the C-terminal region is likely mediated by multiple interactions and may include a potential glycine dimerization motif as well as a leucine zipper dimerization motif that partially spans the C-terminal transmembrane domain [18]. Mutation of all leucine residues within the leucine zipper motif to alanine decreased receptor oligomerization and SR-BI-mediated cholesterol transport [18].

Seeking to gain additional insights into how the C-terminal region of SR-BI contributes to its function, we solved the high-resolution NMR structure of an SR-BI peptide encompassing residues 405–475 [SR-BI(405–475)], which spans the C-terminal transmembrane domain and proximal residues in the extracellular domain [18]. The amino acid sequence and NMR structure of SR-BI(405–475) revealed four conserved proline (Pro/P) residues, including one proline (Pro-459) that induces a kink in the transmembrane α-helix. Proline residues are so-called helix-breakers that generate kinks in α-helices due to the lack of a hydrogen bond donor and steric constraints [25]. Nonetheless, proline residues have been observed in the transmembrane domains of integral membrane proteins [26], albeit less frequently than other amino acids. The role of Pro-459 and the importance of the Pro-459-induced kink in SR-BI function have not yet been described.

In this study, we examined the role of conserved proline residues in SR-BI(405–475) with the goal of better understanding the structural features that contribute to SR-BI-mediated cholesterol transport. We hypothesized that the conserved proline residues support SR-BI in a conformation that allows for efficient cholesterol transport. To test this, we generated four different Pro-to-alanine (Ala/A) mutations in full-length SR-BI receptors (P408A-, P412A-, P438A-, and P459A-SR-BI) and transiently expressed the mutant receptors in COS-7 cells to determine how the mutations affected cholesterol transport. Our findings indicate that SR-BI-mediated cholesterol transport requires key proline residues in the C-terminal region of SR-BI.

Materials and methods

Materials

COS-7 cells were purchased from American Type Culture Collection (ATCC, Manassas, VA). Antibodies targeting SR-BI's C-terminal region (residues 450–509) or extracellular domain (residues 230–380) and anti-microtubule-associated protein 1A/1B-light chain 3B (LC3B) were obtained from Novus Biologicals, Inc. (Littleton, CO). Anti-glyceraldehyde-3-phosphate dehydrogenase (GAPDH) antibody was from Cell Signaling Technology (Danvers, MA). Anti-ubiquitin antibody was from Thermo Fisher Scientific (Waltham, MA). Peroxidase-conjugated anti-rabbit IgG and anti-mouse IgG were obtained from Amersham–GE Healthcare (Chicago, IL). Fluorescein isothiocyanate (FITC)-conjugated anti-rabbit IgG was purchased from BD Biosciences (Franklin Lakes, NJ). Human HDL was purchased from Alfa Aesar (Tewksbury, MA). [^{3}H]-cholesterol and [^{125}I]-sodium iodide were from PerkinElmer (Waltham, MA). [^{3}H]-cholesteryl oleyl ether (COE) was from American Radiolabeled Chemicals, Inc. (St. Louis, MO). Chloroquine diphosphate salt, carbobenzoxy-Leu-Leu-leucinal (MG-132), cholesterol oxidase (Streptomyces), and thin-layer chromatography standards (cholesterol, 4-cholesten-3-one, and cholesteryl oleate) were obtained from Sigma–Aldrich (St. Louis, MO). All other reagents were of analytical grade.

SR-BI expression plasmids

Four Pro-to-Ala mutations were generated at positions 408, 412, 438, or 459 in the coding region of murine SR-BI, which was previously cloned into a pSG5 expression vector [5] (Stratagene, Inc.). Top Gene Technologies (Pointe-Claire, Quebec, Canada) performed cloning, site-directed mutagenesis, and sequencing.

Cell culture and transfection

COS-7 cells were maintained in high-glucose DMEM (Dulbecco's modified Eagle's medium, Gibco) containing 10% (v/v) newborn calf serum, 2 mM L-glutamine, 50 units/ml penicillin, 50 μg/ml streptomycin, and 1 mM sodium pyruvate under standard conditions (37°C/5% CO_2). Upon reaching 60–70% confluency, cells were transiently transfected with cDNA encoding empty pSG5 vector, wild-type (WT), or SR-BI mutant receptors using FuGENE 6 (Promega) at a ratio of 3 : 1 (FuGENE 6:plasmid DNA), as previously described [5]. All experiments were performed 48 h post-transfection unless stated otherwise.

RT-PCR analysis

RNA was isolated using TRIzol (Invitrogen), adhering to the manufacturer's instructions. RT-PCR was performed to assess mRNA expression of SR-BI using the following murine-specific primers (Integrated DNA Technologies): 5′-CCGTCCCTTTCTACTTGTCTG-3′ (forward) and 5′-ACCTTTTGTCTGAACTCCCTG-3′ (reverse). Samples were separated on 2% agarose gels containing ethidium bromide and visualized on an AlphaImager (Alpha Innotech).

Cell lysis

Total cellular proteins were harvested by incubation in radioimmunoprecipitation assay (RIPA) buffer (1% NP-40, 10 mM Tris [pH 8.0], 150 mM NaCl, 0.5% sodium deoxycholate, and 0.1% SDS) containing protease inhibitors (1 μg/ml pepstatin/leupeptin/aprotinin and 20 μg/ml phenylmethylsulfonyl fluoride), and the resulting lysates were cleared by centrifugation at 6010×***g***. Protein concentrations were determined by the Lowry method [27].

Immunoblot analysis

Cellular lysates (10–20 μg protein) were separated by 8%, 10%, or 12% SDS–PAGE and transferred to nitrocellulose or polyvinylidene difluoride membranes which were then blocked in 5% nonfat dry milk (w/v) in 1× Tris-buffered saline with 0.05% Tween-20 (TBST). Antibody incubations were performed in 1% milk/TBST at the following dilutions: C-terminal region of SR-BI (1 : 5000), GAPDH (1 : 5000), ubiquitin (1 : 1000), LC3B (1 : 1000), peroxidase-conjugated donkey anti-rabbit IgG (1 : 10 000), and peroxidase-conjugated sheep anti-mouse IgG (1 : 10 000). Bands were detected upon exposure to SuperSignal West Pico or SuperSignal West Pico PLUS (Thermo Fisher Scientific) chemiluminescent substrate.

SR-BI cell surface staining and flow cytometry

Cells expressing empty vector, WT, or mutant SR-BI receptors were trypsinized, resuspended in DMEM, and centrifuged at 300×***g***. Pellets were then washed in phosphate-buffered saline (PBS) containing 0.5% bovine serum albumin (BSA) and incubated with anti-extracellular SR-BI antibody (1 : 100) for 1 h on ice. Cells were washed and incubated with FITC-conjugated anti-rabbit IgG (1 : 200) for 20 min on ice. After a final wash, cell pellets were resuspended in PBS/0.5% BSA, and 10 000 events were recorded on an Accuri C6 flow cytometer (BD Biosciences; Blood Research Institute, Medical College of Wisconsin) equipped with a 488 nm laser. Analysis was performed using CFlow Plus software (BD Biosciences). Live cell populations (gated from the forward vs. side scatter plot) were further gated into FITC-positive populations by arbitrarily setting empty vector-transfected cells such that ∼3% of cells were positive for FITC. Mean fluorescence intensity (MFI) of FITC-positive cells was obtained for each sample, and MFI of the secondary antibody-only control was subtracted from each sample to account for background staining. MFI for each sample was set relative to average WT-SR-BI levels from all transfections.

Proteasomal/lysosomal degradation studies

For proteasome inhibition experiments, cells expressing empty vector, WT-, or P408A-SR-BI were incubated with culture media containing 0, 3, 6, or 15 μM MG-132 for 24 h at 37°C. For lysosomal degradation studies,

Biochemical Journal (2019) 476 951–963
https://doi.org/10.1042/BCJ20180831

cells expressing empty vector, WT-, or P408A-SR-BI were treated with chloroquine (0, 10, 30, or 100 μM) for 16 h at 37°C. Following incubation with the inhibitors, cellular proteins were harvested in RIPA buffer and subjected to SDS–PAGE and immunoblot analysis for detection of SR-BI protein or control proteins (GAPDH, β-actin, ubiquitin, and LC3B), according to the protocols described above.

HDL cell association and uptake of CE

Human HDL was double-radiolabeled with [^{3}H]-COE and [^{125}I] using recombinant CE transfer protein (Roar Biomedical) and dilactitol-tyramine, respectively, according to established methods [28]. Cellular association of [^{125}I]-HDL and uptake of [^{3}H]-COE were assayed as previously described [28]. Radioactivity measurements were normalized to corresponding sample protein concentrations, as determined by the Lowry method, as well as specific activity of each radioisotope [specific activities of HDL preparations (mean ± SEM, standard error of the mean): [^{125}I] = 221.6 ± 21.2 DPM/ng protein, [^{3}H]-COE = 619.6 ± 7.2 DPM/ng protein].

Cholesterol oxidase sensitivity assay

Immediately after seeding onto 12-well plates, cells transiently expressing empty vector, WT-, or mutant SR-BI receptors were pre-radiolabeled in DMEM containing 2 μCi/ml [^{3}H]-cholesterol and 1 μg/ml acyl-CoA:cholesterol acyltransferase (ACAT) inhibitor (Sigma–Aldrich) for 24 h at 37°C. Cholesterol oxidase sensitivity assays were performed by washing excess [^{3}H]-cholesterol with PBS and incubating cells in DMEM/0.5% BSA containing 0.5 U/ml cholesterol oxidase and 1 μg/ml ACAT inhibitor for 4 h at 37°C. Cellular lipids were extracted with isopropanol, mixed with standards (cholesterol, cholestenone, and cholesterol oleate), separated on thin-layer chromatography paper (Agilent Technologies) using a solvent mixture of 180 hexanes : 20 ethyl ether : 2 methanol (v/v/v), and lipids were visualized by exposure to iodine. Radioactivity corresponding to each lipid species was measured on a Tri-Carb 2100TR liquid scintillation counter (PerkinElmer).

Efflux of free cholesterol

Cells transiently expressing empty vector, WT-, or mutant SR-BI receptors were pre-radiolabeled with [^{3}H]-cholesterol, as described above. Media were replaced with DMEM/0.5% BSA 48 h post-transfection, and cholesterol efflux assays were performed 72 h post-transfection. Cells were incubated with 50 μg/ml human HDL and 1 μg/ml ACAT inhibitor in DMEM/0.5% BSA for 4 h at 37°C. Media were collected, centrifuged at 1500×***g***, and supernatants were subjected to scintillation counting. After washing the cells with PBS, the remaining cellular lipids were extracted using isopropanol, and radioactivity was measured by scintillation counting.

Oligomerization studies

Cells expressing empty vector, WT-, or mutant SR-BI were harvested in PBS containing protease inhibitors (1 μg/ml pepstatin/leupeptin/aprotinin and 20 μg/ml phenylmethylsulfonyl fluoride) with gentle scraping and sonicated briefly on ice for four cycles. Lysates (10 μg protein) were incubated with perfluorooctanoic acid (PFO) sample buffer (5% PFO, 100 mM Tris base, 20% glycerol, and 0.005% bromophenol blue) for 30 min at room temperature. Samples were loaded on 8% polyacrylamide gels lacking SDS in PFO running buffer (25 mM Tris base, 192 mM glycine, and 0.5% PFO), separated at constant 20 mA, transferred to nitrocellulose membranes, and immunoblotting was performed as described above.

Statistical analysis

P-values with respect to WT-SR-BI activity or expression were calculated using one-way analysis of variance (ANOVA) with Dunnett's or Sidak's multiple comparisons tests, where $^{***}P < 0.001$, $^{*}P < 0.05$, and no significance (ns) $P \geq 0.05$.

Results

SR-BI's C-terminal transmembrane domain and adjacent extracellular regions contain four conserved proline residues

To study the importance of conserved proline residues in SR-BI's C-terminal transmembrane domain and proximal extracellular region, we began by generating multiple-species sequence alignments of SR-BI(405–475) using the Multiple Sequence Comparison by Log-Expectation (MUSCLE) algorithm [29] (Figure 1A). High amino acid conservation was observed for four proline residues (Pro-408, Pro-412, Pro-438, and Pro-459). Of

Biochemical Journal (2019) **476** 951–963
https://doi.org/10.1042/BCJ20180831

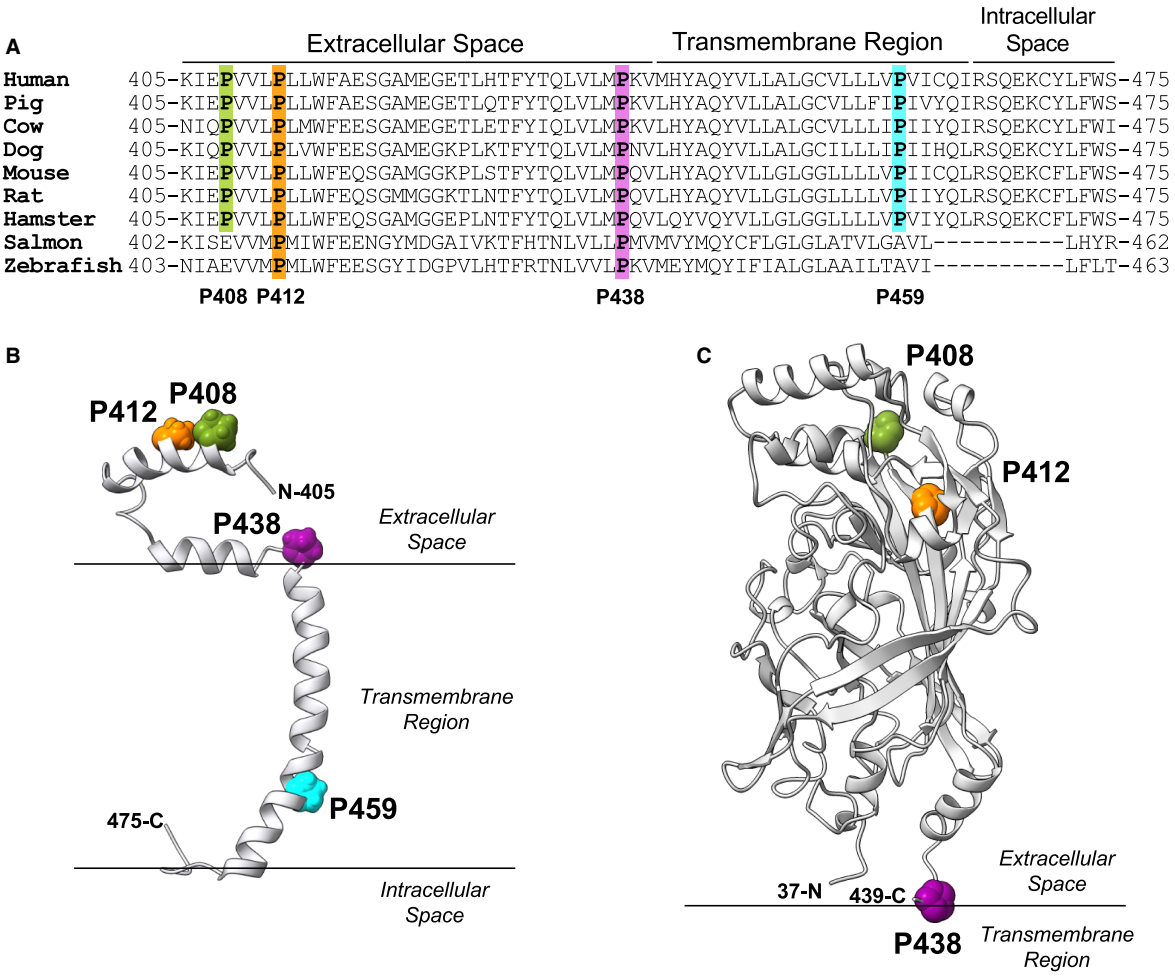

Figure 1. Sequence conservation alignments and structural modeling of proline residues in SR-BI's C-terminal transmembrane domain and proximal extracellular domain.

(**A**) Multiple-species sequence alignments of SR-BI(405–475) were generated using the MUSCLE algorithm. (**B**) NMR structure of SR-BI(405–475) [18] (PDB: 5KTF) is shown, and the locations of conserved proline residues are highlighted as spheres. (**C**) A homology model of SR-BI's extracellular domain was generated using MODELLER [30] with conserved proline residues indicated. Pro-459 is not indicated, as the homology model only represents the extracellular domain.

those, two proline residues (Pro-412 and Pro-438) were fully conserved amongst all species, while Pro-408 and Pro-459 were highly conserved except in lower vertebrates such as salmon and zebrafish. The four conserved proline residues were mapped onto the NMR structure of SR-BI(405–475) (Figure 1B). In the NMR structure, Pro-408, Pro-412, and Pro-438 are located in the extracellular region, while Pro-459 generates a kink in the C-terminal transmembrane domain of SR-BI. For comparison, we mapped Pro-408, Pro-412, and Pro-438 onto a homology model of SR-BI's extracellular domain that was generated with MODELLER software [30] using the X-ray crystal structure of the luminal domain of lysosomal integral membrane protein 2 (LIMP-2) [19] as a template (Figure 1C). In the homology model, Pro-408 and Pro-438 are in flexible linker regions, while Pro-412 is within a β-strand.

Transiently transfected COS-7 cells express WT-, P412A-, P438A-, and P459A-SR-BI at the cell surface

To test the functional importance of conserved proline residues in SR-BI(405–475), we utilized COS-7 cells as an *in vitro* overexpression system. COS-7 cells express a low level of endogenous SR-BI and are amenable to

Biochemical Journal (2019) **476** 951–963
https://doi.org/10.1042/BCJ20180831

transient transfection of plasmids encoding full-length SR-BI. We used various methods to confirm the successful transfection and expression of WT and Pro-to-Ala mutant SR-BI receptors. Robust SR-BI gene expression was verified by RT-PCR for all SR-BI-transfected conditions, while trace amounts of PCR product could be detected for empty vector-transfected cells, likely due to low endogenous SR-BI expression (Figure 2A). SR-BI protein expression in whole-cell lysates was determined by SDS–PAGE and immunoblotting with an antibody directed against the C-terminal region of SR-BI (Figure 2B). Expression of most proline mutants was comparable to WT-SR-BI with the exception of P408A-SR-BI, which showed markedly reduced expression of SR-BI and was only detectable at saturating film exposures (data not shown). The same decrease in P408A-SR-BI expression was observed when using an antibody that targets the extracellular domain of SR-BI, and P408A-SR-BI was not detected in the pellet after centrifugation of the cell lysate (data not shown). As cell surface localization of SR-BI is essential for its interaction with HDL and cholesterol transport functions, we used flow cytometry to analyze the cells that were stained for cell surface SR-BI expression (Figure 2C). We confirmed that all mutant SR-BI receptors (excluding P408A-SR-BI) are present at the plasma membrane of COS-7 cells at levels comparable to WT-SR-BI or greater (in the case of P412A-SR-BI) (Figure 2C). Consistent with total protein analysis, P408A-SR-BI cell surface expression was noticeably lower but did not reach statistical significance (Figure 2C).

Reduced P408A-SR-BI expression is not likely due to proteasomal or lysosomal degradation

Proline residues are involved in the rate-limiting steps of protein folding [31]. We hypothesized that P408A-SR-BI expression is decreased due to a protein folding defect, resulting in a misfolded protein that would be degraded by either the ubiquitin/proteasome system or the lysosome. If WT- or P408A-SR-BI is degraded by these pathways, we would expect SR-BI protein to accumulate in the presence of proteasome or lysosome inhibitors. To assess the proteasomal degradation of SR-BI, 24 h post-transfection with empty vector, WT-, and P408A-SR-BI, cells were treated with 0–15 μM MG-132 for 24 h and analyzed by immunoblotting.

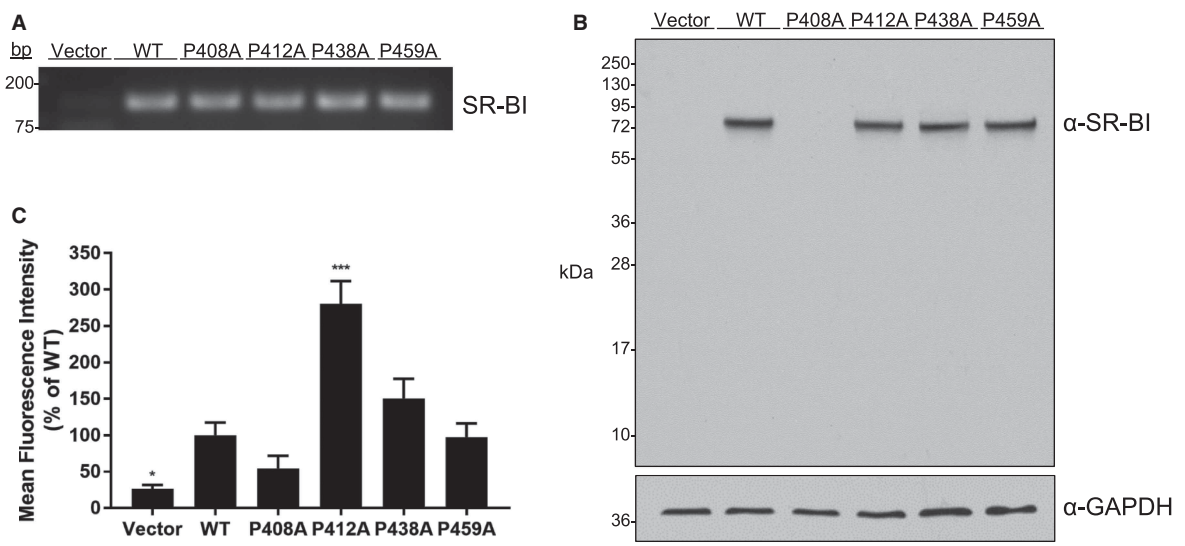

Figure 2. Transiently transfected COS-7 cells express WT-, P412A-, P438A-, and P459A-SR-BI on the cell surface, while P408A-SR-BI protein expression is markedly reduced.

(**A**) RNA was isolated from COS-7 cells expressing empty vector, WT-, or mutant SR-BI for RT-PCR analysis of *SCARB1* (124 bp product) gene expression ($n = 3$). (**B**) Immunoblot analysis of total SR-BI protein expression in transfected COS-7 cells was performed using an antibody directed against the C-terminal region of SR-BI (82 kDa). Total protein expression is assessed for each transfection, and a representative blot is shown ($n = 8$). (**C**) SR-BI cell surface expression was analyzed by flow cytometry using an antibody that recognizes the extracellular domain of SR-BI. MFI was plotted as a percentage of WT-SR-BI expression levels. Data are expressed as mean ± SEM from three to six independent transfections. $^{***}P < 0.001$, $^{*}P < 0.05$ vs. WT-SR-BI, calculated by one-way ANOVA with Dunnett's multiple comparisons test.

Biochemical Journal (2019) **476** 951–963
https://doi.org/10.1042/BCJ20180831

Increased total protein ubiquitination was observed in the presence of MG-132, confirming that proteasomal inhibition was successful (Figure 3A). However, we observed no increase in WT- or P408A-SR-BI in the presence of MG-132 (Figure 3B), suggesting that P408A-SR-BI is not degraded by the proteasome. To assess lysosomal degradation of SR-BI, transfected cells were treated with 0–100 μM chloroquine for 16 h (Figure 3C). Chloroquine inhibition was confirmed by an increase in LC3B-II expression (Figure 3C). Neither WT- nor P408A-SR-BI expression was increased by treatment with chloroquine (Figure 3D). Since cell surface protein expression of P408A-SR-BI appears to be defective, we chose to exclude this mutant from the functional analyses described below.

Cell association of HDL and uptake of CEs are less efficient in cells expressing P412A-, P438A-, and P459A-SR-BI

HDL binds to SR-BI expressed on liver cells, and SR-BI facilitates the transport of HDL-CE into cells for biliary excretion, effectively clearing cholesterol via reverse cholesterol transport. To determine the ability of the proline mutant SR-BI receptors to bind HDL and mediate CE uptake, cells expressing empty vector, WT-, or mutant SR-BI receptors were incubated with [^{125}I]/[^{3}H]-COE-HDL for 1.5 h, as described in Materials and Methods. HDL cell association was decreased to levels of 4.6%, 43%, and 69% relative to WT-SR-BI (100%) in the presence of P412A-, P438A-, and P459A-SR-BI, respectively (Figure 4A). As expected due to the loss of HDL cell association, all three proline mutants also showed decreased [^{3}H]-COE uptake (4.4%, 47%, and 40%, for P412A-, P438A-, and P459A-SR-BI, respectively, vs. WT-SR-BI) (Figure 4B).

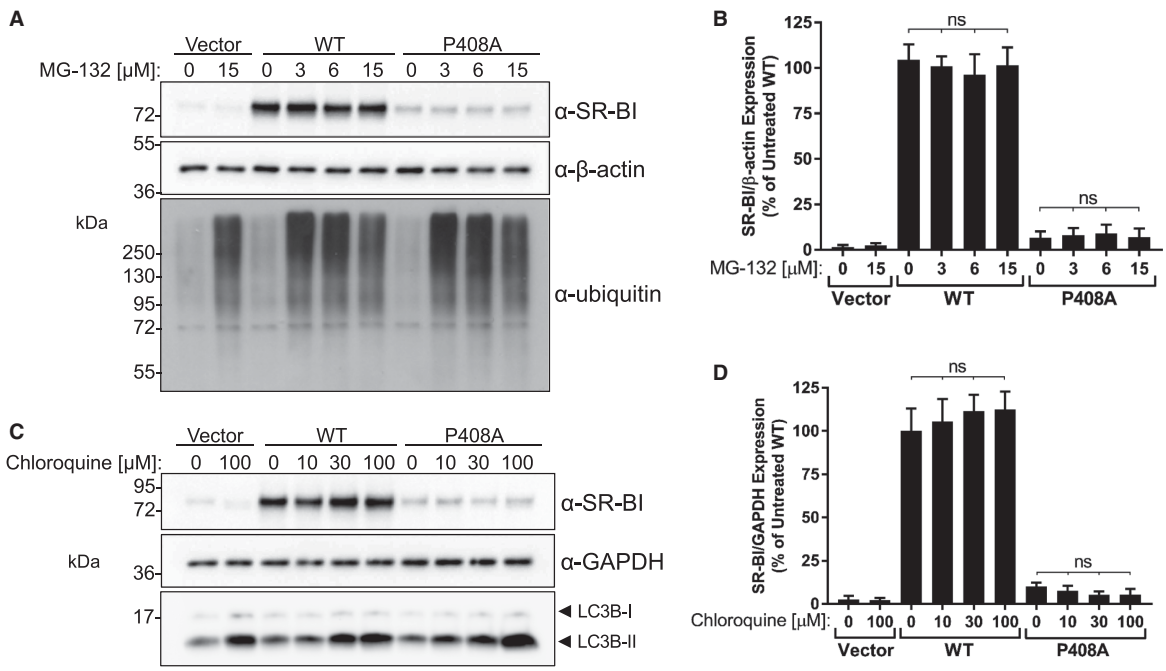

Figure 3. Proteasomal or lysosomal inhibition does not lead to accumulation of WT- or P408A-SR-BI in COS-7 cells.
(**A**) For proteasomal inhibitor assays, COS-7 cells expressing empty vector, WT-, or P408A-SR-BI were treated with 0–15 μM MG-132 for 24 h and then subjected to immunoblot analysis ($n = 3$). Blots were probed with antibodies against the C-terminal region of SR-BI, β-actin (loading control), and ubiquitin (positive control for MG-132 inhibition). (**B**) Relative SR-BI expression was quantified using ImageJ software and expressed as a percentage of untreated WT-SR-BI-expressing cells. (**C**) COS-7 cells expressing empty vector, WT-, or P408A-SR-BI were treated with 0–100 μM chloroquine for 16 h to assess lysosomal degradation ($n = 3$). Blots were probed with antibodies against the C-terminal region of SR-BI, GAPDH (loading control), and LC3B (positive control for chloroquine inhibition). (**D**) SR-BI expression relative to GAPDH (loading control) was quantified, as in (**B**). ns, not significant ($P > 0.05$) between indicated groups as determined by one-way ANOVA using Sidak's multiple comparisons test.

Biochemical Journal (2019) **476** 951–963
https://doi.org/10.1042/BCJ20180831

P412A- and P438A-SR-BI fail to promote accessibility of membrane-free cholesterol to exogenous cholesterol oxidase

SR-BI functions independently of HDL to redistribute membrane cholesterol [32]. To assess the ability of SR-BI to modulate membrane cholesterol distribution, cells transfected with empty vector, WT-, or mutant SR-BI were pre-labeled with [^{3}H]-cholesterol and incubated with exogenous cholesterol oxidase for 4 h, and the resulting lipid species were separated by thin-layer chromatography. Cholesterol oxidase catalyzes the conversion of free cholesterol to cholestenone (Figure 5A). Kellner-Weibel et al. [32] have demonstrated that WT-SR-BI expression increases the production of cholestenone, presumably by modulating membrane cholesterol distribution and increasing accessibility to cholesterol oxidase. Following incubation with cholesterol oxidase, cells expressing P412A-SR-BI were unable to produce cholestenone, while P438A-SR-BI showed ∼76% less [^{3}H]-cholestenone production than cells expressing WT-SR-BI, suggesting that these mutant receptors have impaired ability to redistribute membrane cholesterol (Figure 5B). Interestingly, mutation of Pro-459 did not result in loss of function (Figure 5B).

SR-BI-mediated cholesterol efflux is impaired with P412A- and P438A-SR-BI

The initiating steps of reverse cholesterol transport include SR-BI-mediated cholesterol efflux to HDL particles [3]. Importantly, cholesterol efflux protects against foam cell formation in arterial macrophages [33]. To assess the ability of proline mutants to facilitate cholesterol efflux, cells transfected with empty vector, WT-, or mutant SR-BI were pre-labeled with [^{3}H]-cholesterol and treated with 50 μg/ml HDL for 4 h. Measurements of [^{3}H]-cholesterol levels in the media and in the remaining cellular lipids were used to calculate the percent of cholesterol efflux. As shown in Figure 6, P412A- and P438A-SR-BI effluxed free cholesterol to HDL at statistically lower levels than WT-SR-BI. On the other hand, the ability of P459A-SR-BI to promote free cholesterol efflux to HDL was similar to that of WT-SR-BI.

Proline mutants retain the ability to form homo-dimers and higher-order oligomers

Oligomerization of SR-BI receptors may play an important role in cholesterol transport [21], and dimerization is mediated, at least in part, by the N- and C-terminal transmembrane domains [18,23,24]. To determine if the presence of proline residues in the C-terminal transmembrane domain and adjacent extracellular domain is required for SR-BI's ability to oligomerize, we harvested cell lysates in buffer containing PFO

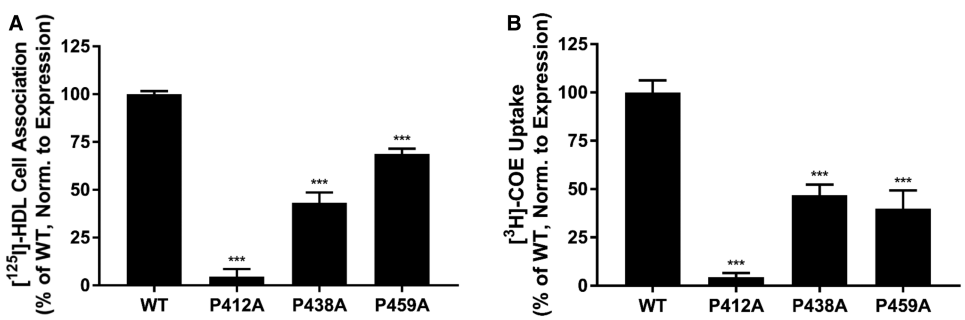

Figure 4. Cell association of HDL and uptake of CEs are less efficient in cells expressing P412A-, P438A-, and P459A-SR-BI.

COS-7 cells expressing empty vector, WT-, or mutant SR-BI receptors were incubated with [^{125}I]/[^{3}H]-COE-HDL (10 μg/ml) for 1.5 h at 37°C. Radioactivity measurements for [^{125}I]-HDL cell association (**A**) and [^{3}H]-COE uptake (**B**) are expressed relative to cell association and uptake in the presence of WT-SR-BI (normalized value = 100%), respectively, after subtracting baseline (empty vector) values. Individual data points are also normalized to cell surface expression data obtained for each independent transfection by flow cytometry of cells plated in parallel wells. Data represent the mean ± SEM of four to seven independent transfections, each performed in triplicate. ***$P < 0.001$ vs. WT-SR-BI, as determined by one-way ANOVA with Dunnett's multiple comparisons test. Raw cell association values (expressed in ng/mg cell protein) were 25.0 ± 2.3 (empty vector) and 78.2 ± 8.0 (WT-SR-BI). Raw uptake values (ng/mg cell protein) were 42.4 ± 4.3 (empty vector) and 69.6 ± 8.7 (WT-SR-BI).

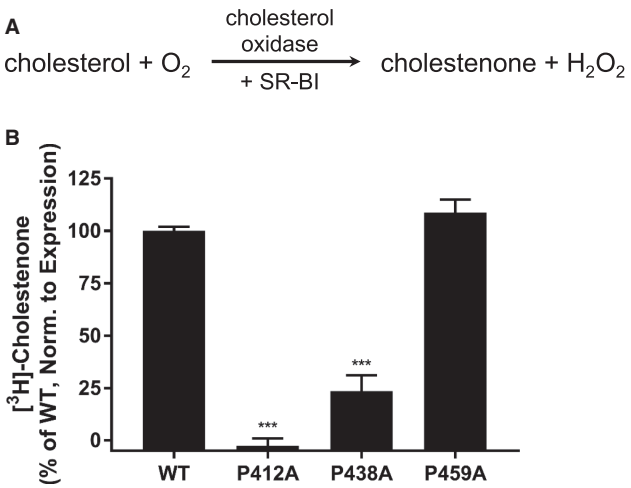

Figure 5. P412A- and P438A-SR-BI fail to promote accessibility of membrane free cholesterol to exogenous cholesterol oxidase.

(**A**) Schematic of the cholesterol oxidase-mediated reaction producing cholestenone, which is enhanced in the presence of WT-SR-BI [32]. (**B**) COS-7 cells transfected with empty vector, WT-, or mutant SR-BI receptors were pre-labeled with [^{3}H]-cholesterol. Following incubation with cholesterol oxidase (0.5 U/ml) for 4 h at 37°C, cellular cholesterol, cholestenone, and CE species were separated by thin-layer chromatography. Radioactivity was measured for each lipid species, and the percentage of cholestenone out of total lipids was calculated and normalized to average WT levels (100%) after subtracting empty vector baseline values. Individual data points are also normalized to cell surface expression data obtained for each independent transfection by flow cytometry of cells plated in parallel wells. Data represent the mean ± SEM for three independent transfections, each performed in quadruplicate. ***$P < 0.001$ vs. WT-SR-BI, as calculated by one-way ANOVA with Dunnett's multiple comparisons test. Raw percentage of cholestenone values are as follows: 9.5 ± 0.6% (empty vector) and 21.8 ± 0.9% (WT-SR-BI).

(a non-dissociative detergent) [34], separated samples by PFO-PAGE, and performed immunoblot analysis using the antibody directed against the C-terminal region of SR-BI. SR-BI dimers and higher-order oligomers were observed for all proline mutants, and the oligomerization profiles all appeared similar to that of WT-SR-BI (Figure 7).

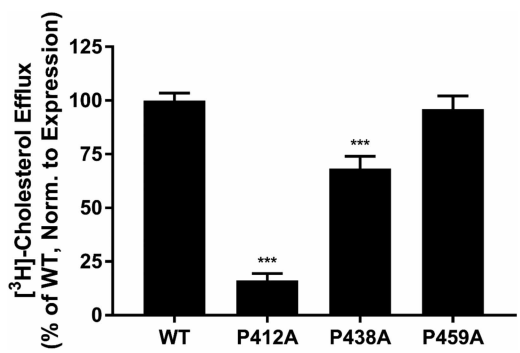

Figure 6. SR-BI-mediated cholesterol efflux is impaired with P412A- and P438A-SR-BI.

COS-7 cells expressing empty vector, WT-, or mutant SR-BI were pre-labeled with [^{3}H]-cholesterol then incubated with HDL (50 μg/ml) for 4 h at 37°C. Media and cellular lipids were analyzed by scintillation counting, and percent efflux was computed (media counts/total lipid counts × 100%) and normalized to mean WT-SR-BI levels after baseline (empty vector) subtraction. Individual data points are also normalized to cell surface expression data obtained for each independent transfection by flow cytometry of cells plated in parallel wells. Data represent the mean ± SEM for five independent transfections, each performed in three to four replicates. ***$P < 0.001$ vs. WT-SR-BI, as determined by one-way ANOVA with Dunnett's multiple comparisons test. Raw percent efflux values are 5.2 ± 0.2% (empty vector) and 7.8 ± 0.5% (WT-SR-BI).

Biochemical Journal (2019) **476** 951–963
https://doi.org/10.1042/BCJ20180831

Discussion

To improve our understanding of the mechanisms underlying SR-BI-mediated cholesterol transport, we applied a structure–function approach, focusing on the functionally relevant C-terminal transmembrane domain and the proximal extracellular domain. Within these regions, we identified four conserved proline residues and assessed the functional importance of each by mutating individual proline residues to alanine. Our results indicate that Pro-412 and Pro-438 are critical for SR-BI-mediated cholesterol transport, Pro-459 is important for HDL cell association and COE uptake, and Pro-408 is required for SR-BI protein expression.

Unexpectedly, we observed a substantial decrease in P408A-SR-BI total protein expression (Figure 2B) without a corresponding decrease in mRNA expression (Figure 2A). Decreased protein expression was verified using antibodies targeting the C-terminal region of SR-BI (Figure 2B) and extracellular domain (data not shown); however, we cannot exclude the possibility that the P408A mutation alters antibody binding. Furthermore, we confirmed that P408A-SR-BI does not separate into the insoluble pellet following cell lysis (data not shown) and is not present as an immature (unglycosylated, 55 kDa) form of the receptor (Figure 2B). Since a key component of protein maturation and folding is proline *cis–trans* isomerization [35], we tested the hypothesis that Pro-408 is a critical mediator of SR-BI folding and that P408A-SR-BI is misfolded and rapidly degraded by either ubiquitin-proteasomal or lysosomal degradation. However, our results do not support the idea that P408A-SR-BI is misfolded and degraded by either of these pathways, as treatment with MG-132 (Figure 3A,B) or chloroquine (Figure 3C,D) does not lead to the accumulation of SR-BI protein. Indeed, it is possible that other protein degradation pathways could be responsible for the low levels of P408A-SR-BI, and this will require further investigation. Otherwise, there may be impairment upstream of protein degradation pathways, potentially at the translational level. Pro-408 is likely not critical for SR-BI expression in all species, as it is not conserved in lower vertebrates such as salmon and zebrafish (Figure 1A). The importance of Pro-408 for SR-BI expression in an *in vivo* system remains to be determined.

The two proline mutants that were defective in all SR-BI-mediated cholesterol transport functions (P412A- and P438A-SR-BI) are also the two most highly conserved proline residues in our study. P412A-SR-BI cell surface expression, as measured by flow cytometry using an extracellular antibody, is increased to ∼280% relative to WT-SR-BI levels (Figure 2C). Although Pro-412 is located outside of the region used to generate the extracellular antibody (residues 230–380), the possibility that P412A mutation disrupts the antibody-binding epitope cannot be ruled out. An increase in P412A-SR-BI expression could be explained as an attempt to compensate for the nonfunctional mutant receptor. Alternatively, increased expression could result from impaired receptor recycling, and this warrants further investigation. Despite seemingly enhanced cell surface expression, P412A-SR-BI remains impaired in its ability to bind HDL, mediate uptake of HDL-CE, efflux free cholesterol, and redistribute membrane cholesterol. Structurally, Pro-412 is located either within an α-helix, as in the NMR structure (Figure 1B), or positioned within a β-strand and oriented

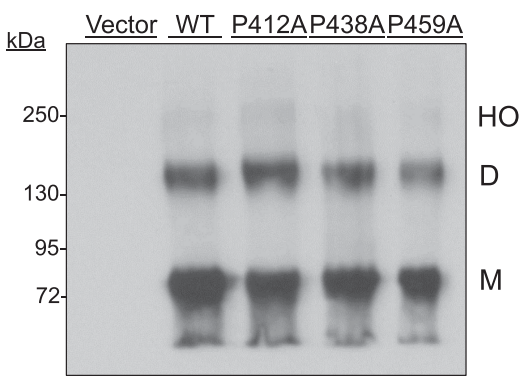

Figure 7. Proline mutants retain the ability to form homo-dimers and -oligomers.

Cell lysates were harvested from COS-7 cells transfected with empty vector, WT-, or mutant SR-BI receptors and separated by PFO-PAGE on 8% polyacrylamide gels. Immunoblot analysis was performed to detect the presence of SR-BI monomers (M), dimers (D), and higher-order (HO) oligomers using an antibody directed against the C-terminal region of SR-BI. Immunoblot is representative of three independent transfections.

away from the core of the extracellular domain, as in the homology model (Figure 1C). The NMR structure may better represent the secondary structure surrounding Pro-412 because it is the only high-resolution structural information for SR-BI. Alternatively, the presence of this α-helix in the NMR structure could be an artifact of determining the structure of only the C-terminal segment of SR-BI in detergent micelles (described in ref. [36]). It remains unknown how mutation of Pro-412 affects SR-BI structure, but short- or long-range conformational changes could disturb the putative hydrophobic channel formed by the β-barrel-like structure (in the homology model) or the nearby three-helix bundle (apex of the homology model). The hydrophobic channel and three-helix bundle are thought to be involved in uptake of CE and HDL cell association, respectively. Pro-438 appears to be in a flexible linker region near the transmembrane domain (Figure 1B,C). If the hydrophobic channel directs cholesterol between the two transmembrane domains, a mutation at the extracellular junction of the C-terminal transmembrane domain could, in theory, impair SR-BI's cholesterol transport functions. Another hypothesis is that Pro-438 forms a flexible kink that enables potential membrane receptor (also known as juxtamembrane) interactions in the adjacent α-helix (residues 426–436) [18]. This hypothesis is currently being investigated by our laboratory. Notably, functional defects with P412A- and P438A-SR-BI are not due to impaired self-association of SR-BI receptors, as both mutants form dimers and higher-order oligomers (Figure 7). The mutant proline receptors were expected to dimerize, as all mutations were made outside of the transmembrane portion of the leucine zipper dimerization motif (residues 413–455).

Mutation of the transmembrane proline kink (Pro-459) to alanine disrupts HDL cell association and HDL-CE uptake, while free cholesterol efflux and membrane cholesterol redistribution are unaffected. It is unknown if HDL binding to SR-BI requires conformational changes involving one or both transmembrane domains, but this could explain why mutation of the flexible proline kink impairs HDL cell association. Despite observing defects in some of SR-BI's cholesterol transport functions, it is possible that the mutant receptor retains the transmembrane kink structure. A similar phenomenon was observed when mutating individual proline kink residues to alanine in bacteriorhodopsin [37]. In addition to forming transmembrane kinks, proline has the unique ability to undergo *cis–trans* isomerization. Proline *cis–trans* isomerization is proposed to act as a molecular switch to regulate signal transduction [38,39]. Therefore, we suspect that other known functions of SR-BI involving signal mechanisms, such as macrophage migration [40] and pro-survival signaling [41], could be impaired in the presence of P459A-SR-BI. It is unknown whether Pro-459 undergoes *cis–trans* isomerization, but we are investigating the hypothesis that conformational changes induced by *cis–trans* isomerization trigger signaling events mediated by SR-BI that lead to the activation of endothelial nitric oxide synthase [42]. In addition, these signaling events require SR-BI's C-terminal transmembrane domain [43], making the transmembrane proline kink an intriguing target for future investigations. SR-BI's N-terminal transmembrane domain also contains a proline residue (Pro-33), although it is predicted to be more proximal to the extracellular space than Pro-459. It is unknown if Pro-33 induces a kink in the N-terminal transmembrane domain or plays a role in SR-BI's athero-protective functions.

Conclusions

Our findings indicate that Pro-412, Pro-438, and, to some extent, Pro-459 are necessary for maintaining SR-BI in a conformation that facilitates proper cholesterol transport. The contribution of these specific proline residues to reverse cholesterol transport *in vivo* remains to be determined. Unexpectedly, we also observed that Pro-408 is required for SR-BI expression. Our findings add to a growing list of structural motifs critical to SR-BI cholesterol transport functions and highlight a previously unstudied proline kink within the C-terminal transmembrane domain of SR-BI.

Abbreviations

ACAT, acyl-CoA:cholesterol acyltransferase; Ala/A, alanine; ANOVA, analysis of variance; BSA, bovine serum albumin; CE, cholesteryl ester; COE, cholesteryl oleyl ether; DMEM, Dulbecco's modified Eagle's medium; FITC, fluorescein isothiocyanate; GAPDH, glyceraldehyde-3-phosphate dehydrogenase; HDL, high-density lipoproteins; LC3B, microtubule-associated protein 1A/1B-light chain 3B; MFI, mean fluorescence intensity; MG-132, carbobenzoxy-Leu-Leu-leucinal; NMR, nuclear magnetic resonance; PBS, phosphate-buffered saline; PFO, perfluorooctanoic acid; Pro/P, proline; RIPA, radioimmunoprecipitation assay; SEM, standard error of the mean; SR-BI, scavenger receptor-BI; TBST, Tris-buffered saline with 0.05% Tween-20; WT, wild type.

Biochemical Journal (2019) **476** 951–963
https://doi.org/10.1042/BCJ20180831

Author Contribution

S.C.P. and D.S. designed research; S.C.P. performed research; S.C.P. and D.S. analyzed data; S.C.P. and D.S. wrote the manuscript.

Funding

This work was supported by the National Institutes of Health grants R01HL58012 (D.S.) and F31HL138744-01 (S.C.P), with partial support from an American Heart Association grant AHA17PRE33650013 (S.C.P.).

Acknowledgements

The authors thank Kay Nicholson for excellent technical guidance and Darcy Knaack and Hayley Powers for critical review of this manuscript. The authors also thank Dr Brian Volkman for helpful discussions.

Competing Interests

The Authors declare that there are no competing interests associated with the manuscript.

References

1 Mozaffarian, D., Benjamin, E.J., Go, A.S., Arnett, D.K., Blaha, M.J., Cushman, M. et al. (2016) Heart Disease and Stroke Statistics—2016 update: a report from the American Heart Association. *Circulation* **133**, e38–e360 https://doi.org/10.1161/CIR.0000000000000350

2 Glass, C.K. and Witztum, J.L. (2001) Atherosclerosis. The road ahead. *Cell* **104**, 503–516 https://doi.org/10.1016/S0092-8674(01)00238-0

3 Glomset, J.A. (1968) The plasma lecithins:cholesterol acyltransferase reaction. *J. Lipid Res.* **9**, 155–167 PMID:4868699

4 Ji, Y., Jian, B., Wang, N., Sun, Y., Moya, M.L., Phillips, M.C. et al. (1997) Scavenger receptor BI promotes high density lipoprotein-mediated cellular cholesterol efflux. *J. Biol. Chem.* **272**, 20982–20985 https://doi.org/10.1074/jbc.272.34.20982

5 Connelly, M.A., Klein, S.M., Azhar, S., Abumrad, N.A. and Williams, D.L. (1999) Comparison of class B scavenger receptors, CD36 and scavenger receptor BI (SR-BI), shows that both receptors mediate high density lipoprotein-cholesteryl ester selective uptake but SR-BI exhibits a unique enhancement of cholesteryl ester uptake. *J. Biol. Chem.* **274**, 41–47 https://doi.org/10.1074/jbc.274.1.41

6 Acton, S., Rigotti, A., Landschulz, K.T., Xu, S., Hobbs, H.H. and Krieger, M. (1996) Identification of scavenger receptor SR-BI as a high density lipoprotein receptor. *Science* **271**, 518–520 https://doi.org/10.1126/science.271.5248.518

7 Babitt, J., Trigatti, B., Rigotti, A., Smart, E.J., Anderson, R.G., Xu, S. et al. (1997) Murine SR-BI, a high density lipoprotein receptor that mediates selective lipid uptake, is N-glycosylated and fatty acylated and colocalizes with plasma membrane caveolae. *J. Biol. Chem.* **272**, 13242–13249 https://doi.org/10.1074/jbc.272.20.13242

8 Kozarsky, K.F., Donahee, M.H., Glick, J.M., Krieger, M. and Rader, D.J. (2000) Gene transfer and hepatic overexpression of the HDL receptor SR-BI reduces atherosclerosis in the cholesterol-fed LDL receptor-deficient mouse. *Arterioscler. Thromb. Vasc. Biol.* **20**, 721–727 https://doi.org/10.1161/01.ATV.20.3.721

9 Trigatti, B., Rayburn, H., Viñals, M., Braun, A., Miettinen, H., and Penman, M. et al. (1999) Influence of the high density lipoprotein receptor SR-BI on reproductive and cardiovascular pathophysiology. *Proc. Natl Acad. Sci. U.S.A.* **96**, 9322–9327 https://doi.org/10.1073/pnas.96.16.9322

10 Brunham, L.R., Tietjen, I., Bochem, A.E., Singaraja, R.R., Franchini, P.L., Radomski, C. et al. (2011) Novel mutations in scavenger receptor BI associated with high HDL cholesterol in humans. *Clin. Genet.* **79**, 575–581 https://doi.org/10.1111/j.1399-0004.2011.01682.x

11 Vergeer, M., Korporaal, S.J., Franssen, R., Meurs, I., Out, R., Hovingh, G.K. et al. (2011) Genetic variant of the scavenger receptor BI in humans. *N. Engl. J. Med.* **364**, 136–145 https://doi.org/10.1056/NEJMoa0907687

12 Chadwick, A.C. and Sahoo, D. (2012) Functional characterization of newly-discovered mutations in human SR-BI. *PLoS ONE* **7**, e45660 https://doi.org/10.1371/journal.pone.0045660

13 Zanoni, P., Khetarpal, S.A., Larach, D.B., Hancock-Cerutti, W.F., Millar, J.S., Cuchel, M. et al. (2016) Rare variant in scavenger receptor BI raises HDL cholesterol and increases risk of coronary heart disease. *Science* **351**, 1166–1171 https://doi.org/10.1126/science.aad3517

14 Papale, G.A., Nicholson, K., Hanson, P.J., Pavlovic, M., Drover, V.A. and Sahoo, D. (2010) Extracellular hydrophobic regions in scavenger receptor BI play a key role in mediating HDL-cholesterol transport. *Arch. Biochem. Biophys.* **496**, 132–139 https://doi.org/10.1016/j.abb.2010.02.011

15 Papale, G.A., Hanson, P.J. and Sahoo, D. (2011) Extracellular disulfide bonds support scavenger receptor class B type I-mediated cholesterol transport. *Biochemistry* **50**, 6245–6254 https://doi.org/10.1021/bi2005625

16 Kartz, G.A., Holme, R.L., Nicholson, K. and Sahoo, D. (2014) SR-BI/CD36 chimeric receptors define extracellular subdomains of SR-BI critical for cholesterol transport. *Biochemistry* **53**, 6173–6182 https://doi.org/10.1021/bi500706x

17 Holme, R.L., Miller, J.J., Nicholson, K. and Sahoo, D. (2016) Tryptophan 415 is critical for the cholesterol transport functions of scavenger receptor BI. *Biochemistry* **55**, 103–113 https://doi.org/10.1021/acs.biochem.5b00804

18 Chadwick, A.C., Jensen, D.R., Hanson, P.J., Lange, P.T., Proudfoot, S.C., Peterson, F.C. et al. (2017) NMR structure of the C-terminal transmembrane domain of the HDL receptor, SR-BI, and a functionally relevant leucine zipper motif. *Structure* **25**, 446–457 https://doi.org/10.1016/j.str.2017.01.001

19 Neculai, D., Schwake, M., Ravichandran, M., Zunke, F., Collins, R.F., Peters, J. et al. (2013) Structure of LIMP-2 provides functional insights with implications for SR-BI and CD36. *Nature* **504**, 172–176 https://doi.org/10.1038/nature12684

20 Rodrigueza, W.V., Thuahnai, S.T., Temel, R.E., Lund-Katz, S., Phillips, M.C. and Williams, D.L. (1999) Mechanism of scavenger receptor class B type I-mediated selective uptake of cholesteryl esters from high density lipoprotein to adrenal cells. *J. Biol. Chem.* **274**, 20344–20350 https://doi.org/10.1074/jbc.274.29.20344

21 Reaven, E., Cortez, Y., Leers-Sucheta, S., Nomoto, A. and Azhar, S. (2004) Dimerization of the scavenger receptor class B type I: formation, function, and localization in diverse cells and tissues. *J. Lipid Res.* **45**, 513–528 https://doi.org/10.1194/jlr.M300370-JLR200

22 Sahoo, D., Darlington, Y.F., Pop, D., Williams, D.L., and Connelly, M.A. (2007) Scavenger receptor class B Type I (SR-BI) assembles into detergent-sensitive dimers and tetramers. *Biochim. Biophys. Acta* **1771**, 807–817 https://doi.org/10.1016/j.bbalip.2006.03.003
23 Gaidukov, L., Nager, A.R., Xu, S., Penman, M. and Krieger, M. (2011) Glycine dimerization motif in the N-terminal transmembrane domain of the high density lipoprotein receptor SR-BI required for normal receptor oligomerization and lipid transport. *J. Biol. Chem.* **286**, 18452–18464 https://doi.org/10.1074/jbc.M111.229872
24 Sahoo, D., Peng, Y., Smith, J.R., Darlington, Y.F. and Connelly, M.A. (2007) Scavenger receptor class B, type I (SR-BI) homo-dimerizes via its C-terminal region: fluorescence resonance energy transfer analysis. *Biochim. Biophys. Acta* **1771**, 818–829 https://doi.org/10.1016/j.bbalip.2007.04.019
25 Reiersen, H. and Rees, A.R. (2001) The hunchback and its neighbours: proline as an environmental modulator. *Trends Biochem. Sci.* **26**, 679–684 https://doi.org/10.1016/S0968-0004(01)01957-0
26 Ulmschneider, M.B. and Sansom, M.S. (2001) Amino acid distributions in integral membrane protein structures. *Biochim. Biophys. Acta* **1512**, 1–14 https://doi.org/10.1016/S0005-2736(01)00299-1
27 Lowry, O.H., Rosebrough, N.J., Farr, A.L. and Randall, R.J. (1951) Protein measurement with the Folin phenol reagent. *J. Biol. Chem.* **193**, 265–275 PMID:14907713
28 Connelly, M.A., De La Llera-Moya, M., Peng, Y., Drazul-Schrader, D., Rothblat, G.H. and Williams, D.L. (2003) Separation of lipid transport functions by mutations in the extracellular domain of scavenger receptor class B, type I. *J. Biol. Chem.* **278**, 25773–25782 https://doi.org/10.1074/jbc.M302820200
29 Edgar, R.C. (2004) MUSCLE: multiple sequence alignment with high accuracy and high throughput. *Nucleic Acids Res.* **32**, 1792–1797 https://doi.org/10.1093/nar/gkh340
30 Sali, A. and Blundell, T.L. (1993) Comparative protein modelling by satisfaction of spatial restraints. *J. Mol. Biol.* **234**, 779–815 https://doi.org/10.1006/jmbi.1993.1626
31 Wedemeyer, W.J., Welker, E. and Scheraga, H.A. (2002) Proline cis-trans isomerization and protein folding. *Biochemistry* **41**, 14637–14644 https://doi.org/10.1021/bi020574b
32 Kellner-Weibel, G., de La Llera-Moya, M., Connelly, M.A., Stoudt, G., Christian, A.E., Haynes, M.P. et al. (2000) Expression of scavenger receptor BI in COS-7 cells alters cholesterol content and distribution. *Biochemistry* **39**, 221–229 https://doi.org/10.1021/bi991666c
33 Moore, K.J., Sheedy, F.J. and Fisher, E.A. (2013) Macrophages in atherosclerosis: a dynamic balance. *Nat. Rev. Immunol.* **13**, 709–721 https://doi.org/10.1038/nri3520
34 Ramjeesingh, M., Huan, L.J., Garami, E. and Bear, C.E. (1999) Novel method for evaluation of the oligomeric structure of membrane proteins. *Biochem. J.* **342**, 119–123 https://doi.org/10.1042/bj3420119
35 Brandts, J.F., Halvorson, H.R. and Brennan, M. (1975) Consideration of the possibility that the slow step in protein denaturation reactions is due to cis-trans isomerism of proline residues. *Biochemistry* **14**, 4953–4963 https://doi.org/10.1021/bi00693a026
36 Chadwick, A.C., Jensen, D.R., Peterson, F.C., Volkman, B.F. and Sahoo, D. (2015) Expression, purification and reconstitution of the C-terminal transmembrane domain of scavenger receptor BI into detergent micelles for NMR analysis. *Protein Expr. Purif.* **107**, 35–42 https://doi.org/10.1016/j.pep.2014.11.001
37 Yohannan, S., Faham, S., Yang, D., Whitelegge, J.P. and Bowie, J.U. (2004) The evolution of transmembrane helix kinks and the structural diversity of G protein-coupled receptors. *Proc. Natl Acad. Sci. U.S.A.* **101**, 959–963 https://doi.org/10.1073/pnas.0306077101
38 Andreotti, A.H. (2003) Native state proline isomerization: an intrinsic molecular switch. *Biochemistry* **42**, 9515–9524 https://doi.org/10.1021/bi0350710
39 Sansom, M.S. and Weinstein, H. (2000) Hinges, swivels and switches: the role of prolines in signalling via transmembrane alpha-helices. *Trends Pharmacol. Sci.* **21**, 445–451 https://doi.org/10.1016/S0165-6147(00)01553-4
40 Al-Jarallah, A., Chen, X., González, L. and Trigatti, B.L. (2014) High density lipoprotein stimulated migration of macrophages depends on the scavenger receptor class B, type I, PDZK1 and Akt1 and is blocked by sphingosine 1 phosphate receptor antagonists. *PLoS ONE* **9**, e106487 https://doi.org/10.1371/journal.pone.0106487
41 Mineo, C., Yuhanna, I.S., Quon, M.J. and Shaul, P.W. (2003) High density lipoprotein-induced endothelial nitric-oxide synthase activation is mediated by Akt and MAP kinases. *J. Biol. Chem.* **278**, 9142–9149 https://doi.org/10.1074/jbc.M211394200
42 Yuhanna, I.S., Zhu, Y., Cox, B.E., Hahner, L.D., Osborne-Lawrence, S., Lu, P. et al. (2001) High-density lipoprotein binding to scavenger receptor-BI activates endothelial nitric oxide synthase. *Nat. Med.* **7**, 853–857 https://doi.org/10.1038/89986
43 Assanasen, C., Mineo, C., Seetharam, D., Yuhanna, I.S., Marcel, Y.L., Connelly, M.A. et al. (2005) Cholesterol binding, efflux, and a PDZ-interacting domain of scavenger receptor-BI mediate HDL-initiated signaling. *J. Clin. Invest.* **115**, 969–977 https://doi.org/10.1172/JCI23858